HIGH REDSHIFT CO LINE EMISSION: PERSPECTIVES

F. COMBES
DEMIRM, Observatoire de Paris,
61 Av. de l'Observatoire, F-75 014, Paris, France
E-mail: francoise.combes@obspm.fr

Although about a dozen high redshift (z larger than 2) starburst galaxies have been recently detected in the CO lines, spectroscopic detections of molecular gas of very young galaxies are still very difficult. The CO lines are usually optically thick, which limits greatly the increase of emission with redshift, as observed for the dust continuum. However the future instruments (LMT, ALMA, etc..) will allow large progress in this domain, and perspectives are discussed. Computations are based on a simple extrapolation of what is known of starbursting galaxies at lower redshift.

1 Introduction

One of the breakthrough due to recent progress on faint galaxies has been the inventory of the amount of star formation at every epoch (e.g. Madau et al. 1996). The comoving star formation rate appears to increase like $(1+z)^4$ from $z = 0$ to $z = 1$, and then decreases again to the same present value down to $z = 5$. But this relies on the optical studies, i.e. on the UV-determined star forming rates in the rest-frame. If early starbursts are dusty, this decrease could be changed into a plateau (Guiderdoni et al. 1997; Blain et al. 1999). To tackle this problem, independent information must be combined in a coherent picture, such as that coming from the far-infrared and millimeter domains: the cosmic IR and submm background radiation discovered by COBE (e.g. Puget et al. 1996; Hauser et al. 1998) yields an insight on the global past star-formation of the Universe, and the sources discovered at high redshift in the millimeter continuum and lines yield information on the structure of the past starbursts (Smail et al. 1997; Hughes et al. 1998; Barger et al. 1999; Guilloteau et al. 1999).

This review focus on the molecular content of galaxies, that we can deduce from CO lines. Although the submillimeter continuum is more easy to detect at high redshift, it cannot without ambiguity trace the evolution of star formation as a function of redshift, because of identification problems, unknown redshifts, and unknown contribution of AGN. After summarising the present state of knowledge concerning CO emission lines, perspectives are drawn concerning the future surveys that will be conducted with the next generation of millimeter instruments.

2 CO Detections at High Redshift

The detection of highly redshifted millimeter CO lines in the hyperluminous object IRAS 10214+4724 ($z = 2.28$, Brown & Vanden Bout 1992, Solomon et al. 1992), has opened this new field, to explore the history of star formation, and its efficiency. Although the first enormous derived H_2 mass has now been revised (the source is considerably amplified by lensing), it is still surprising to find such huge amounts of CO molecules, especially since the gas is expected to have lower metallicity at high z. But theoretical calculations have shown that in a violent starburst, the metallicity could reach solar values very quickly (Elbaz et al. 1992).

Today, more than a dozen objects have been detected in CO lines at high z: they are often gravitationally amplified, either being multi-imaged by a strong lens, like the Cloverleaf quasar H 1413+117 at $z = 2.558$ (Barvainis et al. 1994), the lensed radiogalaxy MG0414+0534 at $z = 2.639$ (Barvainis et al. 1998), or the possibly magnified object BR1202-0725 at $z = 4.69$ (Ohta et al. 1996, Omont et al. 1996); or they are more weakly amplified by a foreground galaxy cluster, like the submillimeter-selected hyperluminous galaxies SMM02399-0136 at $z = 2.808$ (Frayer et al. 1998), and SMM 02399-0134at 1.062 (Kneib et al. 2000). Often several high-J CO lines are detected, revealing the high temperature of the gas (typical of a starburst at $\sim$ 60K). Higher temperatures are rare, as in the magnified BAL quasar APM08279+5255, at $z = 3.911$, where the gas temperature derived from the CO lines is $\sim$ 200K, maybe excited by the quasar (Downes et al. 1999). Recently Scoville et al. (1997b) reported the detection of the first non-lensed object at $z = 2.394$, the weak radio galaxy 53W002, and Guilloteau et al. (1997) the radio-quiet quasar BRI 1335-0417, at $z = 4.407$, which has no direct indication of lensing. If the non-amplification is confirmed, these objects would contain the largest molecular contents known ($8 - 10 \cdot 10^{10}$ $M_\odot$ with a standard CO/H_2 conversion ratio, and even more if the metallicity is low). The derived molecular masses are so high that H_2 would constitute between 30 to 80% of the total dynamical mass (cf 4C 60.07, Papadopoulos et al. 2000), if the standard CO/H_2 conversion ratio was adopted. The application of this conversion ratio is however doubtful, and it is possible that the involved H_2 masses are 3-4 times lower (Solomon et al. 1997).

To search for primeval galaxies, already Elston et al. (1988) had identified extremely red objects that are conspicuous only in the near-infrared (R - K > 5). Maybe 10% of the submm sources could be EROs (Smail et al. 1999). A proto-typical ERO at z=1.44 (Dey et al. 1999) has been detected in submm continuum (Cimatti et al. 1998), and in CO lines (Andreani et al. 2000).

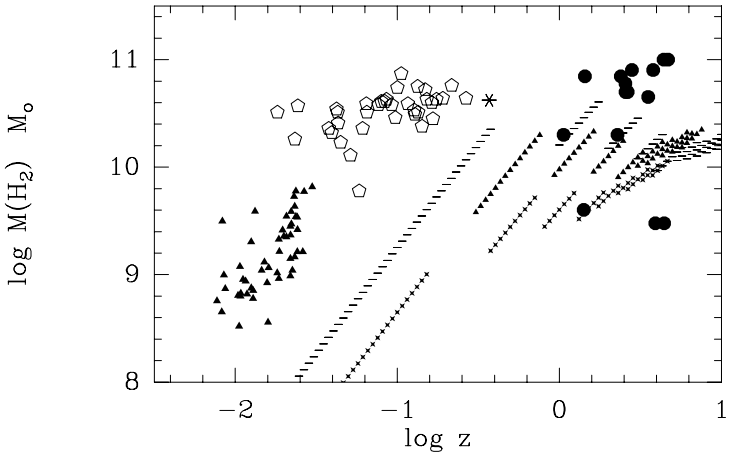

Figure 1. H_2 masses for the CO-detected objects at high redshift (full dots), compared to the ultra-luminous-IR sample of Solomon et al. (1997, open pentagons), to the Coma supercluster sample from Casoli et al (1996, filled triangles), and to the quasar 3c48, marked as a star (Scoville et al. 1993, Wink et al. 1997). The lines delineated by various symbols indicate the 1σ detection limit at the IRAM-30m telescope of S(CO) = 1.0 Jy km/s with the 3mm receiver (hyphens), 2.0 Jy km/s with the 2mm (triangles) and 1.3mm (crosses) receivers, rms that we can reach in 6h integration. Note the absence of detected objects between 0.36 and 1 in redshift. The points at high z can be detected well below the sensitivity limit, since they are gravitationally amplified.

The CO line detections at high z up to now are summarized in Table 1, and the molecular masses as a function of redshift are displayed in Fig. 1. It is clear from this figure that only the very strongest objects are detected, and in particular the gravitationally amplified ones. but this will rapidly change with the new millimeter instruments planned over the world (the Green-Bank-100m of NRAO, the LMT-50m of UMass-INAOE, the ALMA (Europe/USA) and the LMSA (Japan) interferometers). It is therefore interesting to predict with simple models the detection capabilities, as a function of redshift, metallicity or physical conditions in the high-z objects.

3 Perspectives with Future mm Instruments

If so many sources have been detected now in the submillimeter domain at high redshifts, it is because around 1mm, starbursts have a larger apparent flux at $z = 2$ or 3 than $z = 1$. The line emission does not have such a negative

K-correction, since in the low frequency domain, the flux of the successive lines increases roughly as ν^2 (optically thick domain), instead of ν^4 for the continuum. Nevertheless the line emission is essential to study the nature of the object (the AGN-starburst connection for instance), and deduce more physics (kinematics, abundances, excitation, etc..). Given the gas and dust temperatures, the maximum flux is always reached at much lower frequencies than in the continuum, since the lines always reflect the energy difference between two levels; this is an advantage, given the largest atmospheric opacity at high frequencies.

Table 1. CO data for high redshift objects

Source	z	CO line	S mJy	ΔV km/s	MH_2 10^{10} $M_\odot$	Ref
SMM 02399-0134	1.062	2-1	3	500	2*	1
0957+561	1.414	2-1	3	440	0.4*	2
HR10	1.439	2-1	4	400	7	3
F10214+4724	2.285	3-2	18	230	2*	4
53W002	2.394	3-2	3	540	7	5
H 1413+117	2.558	3-2	23	330	2-6 *	6
SMM 14011+0252	2.565	3-2	13	200	5*	7
MG 0414+0534	2.639	3-2	4	580	5*	8
SMM 02399-0136	2.808	3-2	4	710	8*	9
6C1909+722	3.532	4-3	2	530	4.5	10
4C60.07	3.791	4-3	1.7	1000	8	10
APM 08279+5255	3.911	4-3	6	400	0.3*	11
BR 1335-0414	4.407	5-4	7	420	10	12
BR 0952-0115	4.434	5-4	4	230	0.3*	13
BR 1202-0725	4.690	5-4	8	320	10	14

* corrected for magnification, when estimated

Masses have been rescaled to $H_0 = 75$km/s/Mpc. When multiple images are resolved, the flux corresponds to their sum

(1) Kneib et al. (2000); (2) Planesas et al. (1999) (3) Andreani et al. (2000); (4) Solomon et al. (1992), Downes et al. (1995); (5) Scoville et al. (1997b); (6) Barvainis et al. (1994); (7) Frayer et al. (1999); (8) Barvainis et al. (1998); (9) Frayer et al. (1998); (10) Papadopoulos et al. (2000); (11) Downes et al. (1999); (12) Guilloteau et al. (1997); (13) Guilloteau et al. (1999); (14) Omont et al. (1996)

3.1 Predicted Line and Continuum Fluxes

To model high-redshift starburst objects, let us extrapolate the properties of more local ones: the active region is generally confined to a compact nuclear disk, sub-kpc in size (Scoville et al. 1997a), Solomon et al. 1990, 97). The gas is much denser here than in average over a normal galaxy, of the order of 10^4 cm^{-3}, with clumps at least of 10^6 cm^{-3} to explain the data on high density tracers (HCN, CS..). To schematize, the ISM maybe modelled by two density and temperature components, at 30 and 90K (cf. Combes et al. 1999). The total molecular mass considered will be $6 \cdot 10^{10}$ $M_\odot$ and the average column density $N(H_2)$ of 10^{24} cm^{-2}, typical of the Orion cloud center.

Going towards high redshift ($z > 9$), the temperature of the cosmic background T_{bg} becomes of the same order as the interstellar dust temperature, and the excitation of the gas by the background radiation competes with that of gas collisions. It might then appear easier to detect the lines (Silk & Spaans 1997), but this is not the case when every effect is taken into account. To have an idea of the increase of the dust temperature with z, the simplest assumption is to consider the same heating power due to the starburst. At a stationary state, the dust must then radiate the same energy in the far-infrared that it receives from the stars, and this is proportional to the quantity $T_{dust}^6 - T_{bg}^6$, if the dust is optically thin, and its opacity varies in ν^β, with $\beta = 2$. Keeping this quantity constant means that the energy re-radiated by the dust, proportional to T_{dust}^6, is always equal to the energy it received from the cosmic background, proportional to T_{bg}^6, plus the constant energy flux coming from the stars. Since β can also be equal to 1 or 1.5, or the dust be optically thick, we have also considered the possibility of keeping $T_{dust}^4 - T_{bg}^4$ constant; this does not change fundamentally the results.

Computing the populations of the CO rotational levels with an LVG code, and in the case of the two component models described earlier, the predictions of the line and continuum intensities as a function of redshift and frequencies are plotted in Fig. 2.

3.2 Source Counts

To predict the number of sources that will become available with the future sensitivity, let us adopt a simple model of starburst formation, in the frame of the hierarchical theory of galaxy formation. The cosmology adopted here is an Einstein-de Sitter model, $\Omega = 1$, with no cosmological constant, and $H_0 =$ 75 km/s/Mpc, $q_0 = 0.5$.The number of mergers as a function of redshifts can be easily computed through the Press-Schechter formalism (Press & Schechter

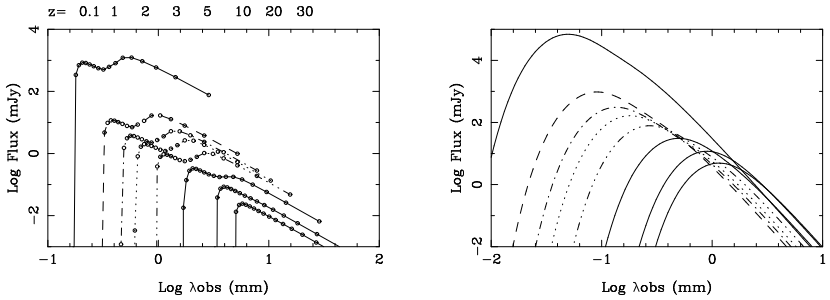

Figure 2. Expected flux for the two-component cloud model, for various redshifts $z = 0.1$, 1, 2, 3, 5, 10, 20, 30, and $q_0 = 0.5$. **Left** are the CO lines, materialised each by a circle (they are joined by a line only to guide the eye). **Right** is the continuum emission from dust. It has been assumed here that $T^6_{\rm dust} - T^6_{\rm bg}$ is conserved (from Combes et al. 1999).

1974), assuming self-similarity for the probability of dark halos merging, and an efficiency of mergers in terms of star-formation peaking at $z \sim 2$ (i.e. Blain & Longair 1993). Also, the integration over all redshifts of the flux of all sources should agree with the cosmic infrared background detected by COBE. These contribute to reduce the number of free parameters of the modelling. To fit the source counts, however, another parameter must be introduced which measures the rate of energy released in a merger (or the life-time of the event): this rate must increase strongly with redshift (cf. Blain et al. 1999). Once the counts are made compatible with the submm observations, the model indicates what must be the contributions of the various redshift classes to the present counts. It is interesting to note that the intermediate redshifts dominate the continuum source counts ($2 < z < 5$), if we allow the star formation to begin before $z = 6$. At higher dust temperature, the counts are dominated by the highest redshifts ($z > 5$).

Once these fits are obtained for the continuum sources, it is possible to derive also the counts for the CO line emission. The spectral energy distribution is now obtained with a comb-like function, representing the rotational ladder, convolved with a Planck distribution of temperature equal to the dust temperature, assuming the lines optically thick. The frequency filling factor is then proportional to the rotational number, and therefore to the redshift, for a given observed frequency. The width of the lines have been assumed to be 300km/s. The derived source numbers are shown in Fig. 3. Note how they are dominated by the high redshift sources. It is not useful to observe at λ

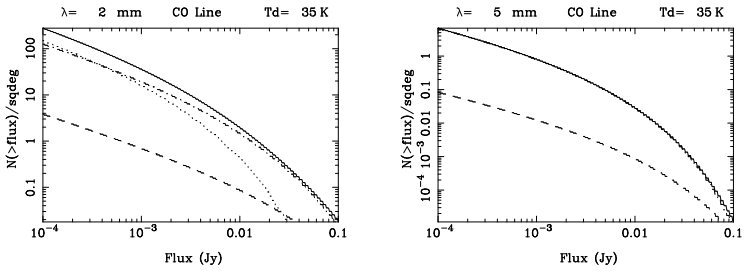

Figure 3. *Left* Source counts for the CO lines at an observed frequency of 2mm, assuming optically thick gas at $T_{ex} = 35$K. The solid line is the total. Dash is the lowest redshifts ($z < 2$); Dot-dash, intermediate ($2 < z < 5$); Dots are the highest redshifts ($z > 5$). *Right* Same for $\lambda = 5$mm.

below 1mm for high-z protogalaxies, but instead to shift towards $\lambda = 1$cm.

4 Conclusion

The search for CO lines in high redshift galaxies is only beginning, there will be a real breakthrough in the next decade, when the sensitivity is increased by more than a factor 10 with the next generation millimeter instruments. CO lines are fundamental for our knowledge of star formation and efficiency at high z, to measure H_2 masses, recognize AGN from starbursts, measure the dynamics and total masses of galaxies.

Acknowledgements

I am very grateful to James Loventhal and David Hughes for the organisation of such an interesting meeting, and to the UMass for their financial help.

References

1. Andreani, P., Cimatti, A., Loinard, L., Rttgering, H.: 2000, A&A 354, L1
2. Barger, A.J., Cowie, L.L., Sanders, D.B.: 1999, ApJ 518, L5
3. Barvainis R., Tacconi L., Antonucci R., Coleman P.: 1994, Nature 371, 586
4. Barvainis R., Alloin D., Guilloteau S., Antonucci R. 1998, ApJ 492, L13
5. Blain A.W., Jameson A., Smail I. et al. : 1999, MNRAS 309, 715
6. Blain A.W., Longair M.S.: 1993, MNRAS 264, 509

7. Brown R., Vanden Bout P.: 1992, ApJ 397, L19
8. Casoli F., Dickey J., Kazes I. et al.: 1996, A&AS 116, 193
9. Cimatti A., Andreani P., Röttgering H., Tilanus R.: 1998, Nature 392, 895
10. Combes F., Maoli R., Omont A.: 1999, A&A 345, 369
11. Dey, A., Graham, J. R., Ivison, R. J. et al.: 1999, ApJ 519, 610
12. Downes D., Neri R., Wiklind T. et al. : 1999, ApJ 513, L1
13. Downes D., Solomon P.M., Radford S.J.E. 1995, ApJ 453, L65
14. Elbaz D., Arnaud M., Casse M., et al.: 1992, A&A 265, L29
15. Elston R., Rieke G.H., Rieke M.J.: 1988, ApJ 331, L77
16. Frayer D.T., Ivison R.J., Scoville N.Z., et al., 1998, ApJ 506, L7
17. Frayer D.T., Ivison R.J., Scoville N.Z., et al., 1999, ApJ 514, L13
18. Guiderdoni B., et al.: 1997, Nature 390, 257
19. Guilloteau S., Omont A., Cox P. et al. 1999, A&A 349, 363
20. Guilloteau S., Omont A., McMahon R.G. et al. 1997, A&A 328, L1
21. Hauser, M. et al., 1998, ApJ 508, 25
22. Hughes D.H., Serjeant S., Dunlop J. et al.: 1998, Nature 394, 241
23. Kneib J-P., Prieur J-L., Ivison R., Smail I., Blain A.: 2000, A&A in prep
24. Madau, P., Ferguson, H. C., Dickinson, M. E., et al. : 1996, MNRAS 283, 1388
25. Ohta K., Yamada T., Nakanishi K., et al.:1996, Nature 382, 426
26. Omont A., Petitjean P., Guilloteau S. et al. 1996, Nature 382, 428
27. Papadopoulos P.P., Rottgering H.J.A., van der Werf P.P., et al. 2000 ApJ. 528, 626
28. Planesas, P., Martin-Pintado, J., Neri, R., Colina, L.: 1999 Science 286, 2493
29. Press W.H., Schechter P.: 1974, ApJ 187, 425
30. Puget, J.-L., Abergel, A., Bernard, J.-P., et al. : 1996, A&A 308, L5
31. Scoville N.Z., Padin S., Sanders D.B. et al. : 1993, ApJ 415, L75
32. Scoville N.Z., Yun M.S., Bryant P.M.: 1997a, ApJ 484, 702
33. Scoville N.Z., Yun M.S., Windhorst R.A. et al. 1997b, ApJ 485, L21
34. Silk J., Spaans M.: 1997, ApJ 488, L79
35. Solomon P.M., Radford S.J.E., Downes D.: 1990, ApJ 348, L53
36. Solomon P.M., Downes D., Radford S.J.E.: 1992, Nature 356, 318
37. Solomon P.M., Downes D., Radford S.J.E., Barrett J.W.: 1997, ApJ 478, 144
38. Smail, I., Ivison, R.J., Blain, A.W., 1997, ApJ, 490, L5
39. Smail, I., Ivison, R.J., Kneib, J-P., et al.: 1999, MNRAS 308, 1061
40. Wink J.E., Guilloteau S., Wilson T.L., 1997, A&A 322, 427